



## Decolorization and mineralization of azo dye Acid Blue 113 by the UV/Oxone process and optimization of operating parameters

Hung-Yee Shu\*, Ming-Chin Chang, Shi-Wei Huang

*Institute of Environmental Engineering, Hungkuang University, Taichung 433, Taiwan, Tel. +886 426318652; ex. 1115; email: hyshu@sunrise.hk.edu.tw (H.-Y. Shu), Tel. +886 426318652, ex. 4113; email: chang@sunrise.hk.edu.tw (M.-C. Chang), Tel. +886 426318652, ex. 4123; love85262@yahoo.com.tw (S.-W. Huang)*

Received 31 January 2015; Accepted 10 March 2015

### ABSTRACT

A UV/Oxone advanced oxidation process was proposed to degrade and mineralize a synthesized Acid Blue 113 (AB113) dyeing wastewater. Various operating parameters which affected the removal efficiencies of AB113 and total organic carbon (TOC) such as reaction time, Oxone dosage, initial AB113 concentration, initial pH, and UV intensity were studied. Results presented effective removal of AB113 azo dye by UV/Oxone process based on both AB113 and TOC indicators. The reaction kinetics was shown to be pseudo-second-order reaction. In UV/Oxone process, the higher the Oxone dosage applied, the higher the AB113 and TOC removal efficiencies can be obtained up to 6.3 mM Oxone concentration. The AB113 removal efficiency and pseudo-second-order rate constant decreased with increase in the initial dye concentration. However, the proposed UV/Oxone process was proved to be able to degrade high AB113 concentration up to 400 mg l<sup>-1</sup>. The initial pH showed no significant effect on AB113 removal efficiency. UV intensity affected TOC mineralization efficiency significantly. In contrast, UV intensity presented less important factors on degradation of AB113.

*Keywords:* Azo dye; Peroxymonosulfate; Oxone; UV irradiation; Sulfate radicals; Decolorization; Mineralization

### 1. Introduction

In Taiwan, textile industry is a traditional but very important industrial category which utilizes about 250 textile dyeing and processing factories and contributes 3.8% of Taiwan total export revenue (11,702 million USD, reported for the year 2013) [1]. However, serious environmental threat caused by huge discharge flow

rate and barely complied water quality is a major concern of this industry. Since dye stuffs used in textile industry are designed to be refractory and hard to destroy by different environmental conditions and biological activities, thus, this effluent is very difficult to be decolorized and mineralized. In order to respond the concerns of public and environmental organizations, Taiwan Environmental Protection Agency enforced the National Effluent Standard of textile

\*Corresponding author.

*Presented at the 7th International Conference on Challenges in Environmental Science and Engineering (CESE 2014) 12–16 October 2014, Johor Bahru, Malaysia*

industry to meet the 550 true color units of American Dye Manufactures Institute (ADMI) by the year 2003 [2]. This regulation enforcement gives textile industry the motivation to take action on more efficient pre-treatment or polishing processes to solve wastewater discharge problems. At the same time, textile industries around the world encounter more or less the same environmental regulation enforcement issues. Therefore, research communities and industries around the world urgently contribute to develop new treatment technologies to resolve dyeing related industrial wastewater problems [3–7]. The target compound Acid Blue 113 (AB113) is categorized as azo dye (with nitrogen double bond,  $-N=N-$ ) which is the largest category of commercial dyes used in textile industry. Furthermore, many researchers are interested in this category azo dye and reported many successful approaches to degrade and decolorize azo dye compounds by various novel technologies [8–11].

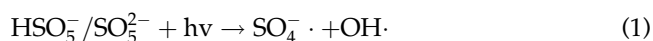
In general, wastewater discharged from dyeing process contains certain amount of residual dyestuffs causing high chemical oxygen demand, high color, and low biodegradability. And this wastewater is usually discharged to the traditional treatment facility utilizing coagulation and activated sludge processes. The coagulation process can hardly remove dyestuff caused color but produces coagulation sludge which needs further disposal. Recently, the disposal cost of sludge raises high which suffers textile industries. Furthermore, dyestuffs are made to be refractory and non-biodegradable. Thus, activated sludge process performs low treatment efficiency caused by dyestuff's complicate property and toxicity which cause recalcitrant to the microorganisms. To increase the color treatment efficiency, some wastewater treatment operators add perchlorate to decolorize dyeing wastewater. However, use of perchlorate causes the formation of carcinogenic chlorinated organic compounds [2]. Thus, to proper treat dyeing wastewater, more advanced and novel technologies are needed.

Advanced oxidation processes (AOPs) are widely studied technologies to decompose all kinds of refractory pollutants. In general, AOPs exercise UV irradiation, ozone, hydrogen peroxide, Fenton reagents and  $TiO_2$ ,  $ZnO$  photocatalysts combinations to form hydroxyl radicals for degradation of recalcitrant pollutants. By formation of the most powerful oxidant, hydroxyl radicals, AOPs present the capability to mineralize most of the organic pollutants into carbon dioxide and water. The applications of AOPs for dyestuffs treatment have revealed successfully to decolorize and mineralize azo dye wastewater by UV/ $H_2O_2$  [12–14], UV/ $O_3$  [15] and Fenton reaction

[4,16]. Photocatalytic processes employing  $TiO_2$  and  $ZnO$  catalysts with UV irradiation are also presented to be effective in decolorizing azo dye wastewater [17–20].

Alternatively, another sulfate radicals ( $SO_4^{\cdot-}$ )-based AOPs (SR-AOPs) are also developed for degradation of organic pollutants. SR-AOPs are increasingly extending importance as *in situ* chemical oxidation (ISCO) technologies for soil and groundwater remediation of contaminants [21–24]. In SR-AOPs, peroxymonosulfate (PMS) or persulfate (PS) is the major oxidant which can be transformed into sulfate radicals with more powerful oxidation potential to degrade refractory pollutants in groundwater or soil through thermal or chemical activation, that is, by UV irradiation, transition metal [23,25–27]. With success of ISCO soil and groundwater remediation, SR-AOPs are emerging applied to the wastewater treatment purpose, recently.

The sulfate radicals are relatively more stable and selective than hydroxyl radicals in aqueous [28]. PMS or PS will produce sulfate radicals with very high redox potential through UV, ultrasound, thermal, and transition metal activation [29–31]. Sulfate radical and hydroxyl radical are both strong oxidants with similar oxidation power presented by redox potential of 2.6 V and 2.8 V, respectively. Studies of SR-AOPs utilizing PMS are mainly focused on transition metal activation processes, recently. Among transition metal, cobalt ion is recognized to be best activator [29,31]. However, cobalt ion after AOPs treatment will be released to the environment and may cause human and environment threat. On the other hand, UV irradiation adds no chemical into the environment and is capable to activate PMS to form sulfate radicals which may be a better and environmental friendly approach as SR-AOPs. PMS anion can be UV photo-activated to form sulfate radicals as presented as follows:



In this study, the degradation of azo dye C.I. AB113 using a recirculated annular cylindrical photoreactor in which the UV 254 lamp irradiation on commercial available PMS, that is, Oxone, to produce sulfate radicals was investigated. Operating parameters such as Oxone dosage, initial dye concentration, initial pH, and UV intensity that may affect the degree of the dye degradation and mineralization were studied. Changes in AB113 concentration, ADMI color unit, total organic carbon (TOC), pH, oxidation reduction potential (ORP) were monitored.

## 2. Materials and methods

### 2.1. Materials and apparatus

C.I. AB113, a dis-azo dye, was tested as model compound for this UV/Oxone decolorization study. AB113 was purchased from Sigma-Aldrich, Inc. and used without further purification. Its chemical properties were summarized as molecular formula of  $C_{32}H_{21}N_5Na_2O_6S_2$ , C.I. 26360, characterized wavelength at 566 nm, molecular weight of  $681.66 \text{ g mole}^{-1}$ , and 50% purity. In general, AB113 is applied widely in various textile dyeing industries to dye wool, silk, and polyamide fiber from a neutral or acid bath. On the other hand, the chemical structure of AB113 can be obtained from our previous study [10]. Reagent grade PMS ( $2KHSO_5 \cdot KHSO_4 \cdot K_2SO_4$ , molecular weight of  $614.78 \text{ g mole}^{-1}$ ), commercial name of Oxone, was purchased from Sigma-Aldrich, Inc. as well.

A recirculated annular cylindrical photoreactor equipped with a low-pressure mercury arc UV lamp (Philippmade, wavelength 253.7 nm, input power of 30 W, 85 cm length) was conducted in the experiments. The photoreactor setup was also presented in our previous work [32]. In this reactor, at center, a UV lamp was protected by central inner quartz tube. And AB113 wastewater was pumped through the thin gap between quartz tube and outer stainless shell. The inside diameter of stainless shell was designed to be 3.20 cm. And the outside diameter of the quartz tube was 2.2 cm. Thus, the annular gap size was 0.5 cm. While AB113 wastewater flowed through the reactor from its inlet to outlet, the effluent was then recirculated back to the stirred storage tank, then, again pumped back to the photoreactor continuously. The UV 254 nm intensity was measured by a UVP made UV radiometer. The UV light intensity of 30 W yielded a surface light energy of  $5.6 \text{ mW cm}^{-2}$  measured at the outer surface of quartz tube. A 1,000 ml dye solution was introduced to the photoreactor and recirculated during the reaction. The temperature was monitored to be slightly increased around room temperature ( $21.4\text{--}25.8^\circ\text{C}$ ) which can influence the reaction kinetics insignificantly.

### 2.2. Experimental procedure and analysis

AB113 solution at various concentrations (mainly  $50 \text{ mg l}^{-1}$ ) was prepared with deionized water. The experimental variables studied included reaction time, Oxone dosage, initial dye concentration, initial pH, and UV intensity. At a predetermined reaction time, an aliquot of the solution was withdrawn and analyzed for residual AB113 concentration, TOC and

ADMI index, pH and redox potential (ORP). In the case of pH effect study, the experiments were conducted by adjusting the initial pH value of 5.8 to the range of 2–10 using HCl and/or NaOH with initial AB113 concentration of  $50 \text{ mg l}^{-1}$  and Oxone dosage 6.3 mM. AB113 concentration was measured by determining the absorbance at characterized wavelength of 566 nm using a Hitachi U-2000 spectrophotometer. TOC was determined with a TOC Analyzer from O.I. Analytical Aurora, model 1030. Color intensity was determined based on the ADMI standard color measurement by applying the Adams–Nickerson color difference formula following method 2120E of the standard methods. The pH and ORP were monitored by a Ea Eutech PH5500 dual channel pH/ion meter with specific probes.

## 3. Results and discussion

### 3.1. Fundamental of UV/Oxone process for degradation of AB113

Oxone is known as a strong oxidant that upon UV irradiation can generate sulfate radicals, very strong oxidant, which can oxidize and decompose a wide group of organic pollutants non-specifically. In this work, the results from Fig. 1(a) indicate that the UV/Oxone system is able to remove AB113 with a superior performance. The results show that about 80% AB113 removal can be reached in 2 min and almost 100% removal is obtained in 30 min of reaction time. From same figure, ADMI color index changes from original 22,179 color units to 2,106 color units in 2 min and further decolorizes to only 70 color units in 60 min. The TOC is an indicator of mineralization. Because of complicated structure and large molecular weight, AB113 resists to be oxidized by sulfate radicals. Thus, at beginning of the oxidation reaction, solution TOC cannot be destroyed easily. At this time region, large molecules were degraded into lower molecule weight intermediates which still contributed to TOC measurement. Therefore, at first 20 min, TOC removal may remain almost unchanged. After this lag phase (20 min), TOC can be removed significantly. The mineralization of AB113 solution by sulfate radicals is rather difficult than that of AB113 degradation, which takes 90 min to obtain  $3.48 \text{ mg l}^{-1}$  residual TOC in comparison with the original TOC of  $19.55 \text{ mg l}^{-1}$  (82.21% TOC removal).

It is interesting to observe that the pH decreases toward acidic condition during the UV/Oxone oxidation. As shown in Fig. 1(b), the pH value of UV/Oxone system drops significantly from initially pH 5.8–3.0 in first 2 min, then, continuously decreases to

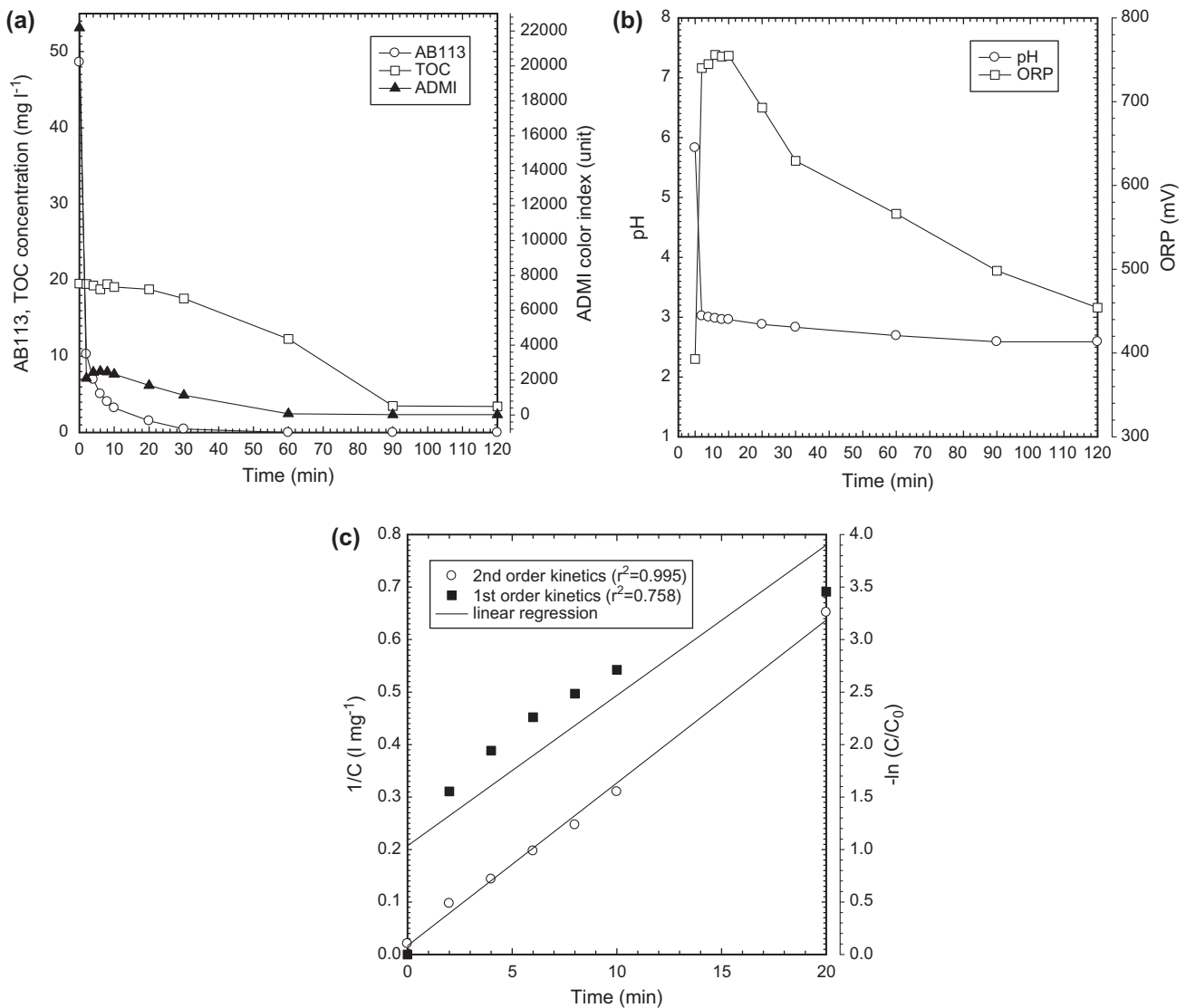


Fig. 1. Indicators monitored during UV/Oxone degradation of AB113 wastewater. (a) AB113, TOC, and ADMI color index, (b) pH and ORP, and (c) first- and second-order kinetics fittings. The conditions were initial dye concentration of 50 mg l<sup>-1</sup>, sodium persulfate dosage 4.2 mM, UV dosage 30 W l<sup>-1</sup>, and reaction time during 120 min.

2.6 at the end of the reaction. This is due to the formation of organic acid byproducts and sulfate ions.

ORP is an important parameter which should be monitored during AOP reaction. High positive values of solution ORP can be obtained for UV/Oxone process as shown in Fig. 1(b). From the figure, the original ORP is 392.8 mV and it increases sharply after UV irradiation to 754.8 mV in first 2 min. This observation explicates that UV/Oxone process is a very powerful oxidative decolorization approach due to the formation of sulfate radicals. During the reaction, the ORP increases to the highest 754.8 mV, then, sharply

decreases to 629.4 mV at 30 min. After 30 min of reaction, the Oxone concentration is exhausted and ORP drops gradually down to 454.2 mV to express the loss of reactivity.

The solution ORP is a measure of the oxidizing or reduction power of the solution. In an oxidizing environment with presence of an oxidizing reagent, such as sulfate radicals, a higher positive ORP value will be observed [33]. Kim et al. reported the use of ORP measurement and control to ensure the wastewater treatment efficiency by Fenton process. They demonstrated an increase of ORP from 560 to 640 mV by addition of

Fenton's reagent. After the reaction, the ORP decreased due to the depletion of Fenton's reagent to produce OH radicals [34].

Fig. 1(c) change and curve fitting for the pseudo-first-order and pseudo-second-order rate expression by using  $-\ln(C/C_0)$  and  $1/C$  vs. time curves. Because the AB113 concentration drops sharply at first 2 min, thus, pseudo-first-order curve fitting shows two segments of linear lines before and after 2-min time. It makes the AB113 degradation data not agree well with pseudo-first-order kinetics ( $r^2 = 0.758$ ). In most of AOPs study, the reaction kinetics can be simplified as pseudo-first-order. However, in this study, it is not suitable to assume first order. On the other hand, the curve fitting for pseudo-second-order presents very good fitting, implies the reaction kinetics is more consistent with second order kinetics ( $r^2 = 0.995$ ).

### 3.2. Effect of Oxone dosage

The experimental conditions were prepared at AB113 initial concentrations of  $50 \text{ mg l}^{-1}$ , Oxone dosage of 0.21–6.3 mM and  $30 \text{ W l}^{-1}$  UV light dosage for a period of 120 min to evaluate the effect of Oxone dosage on this UV/Oxone system.

Fig. 2(a) shows the removal of AB113 as a function of Oxone dosage under  $30 \text{ W l}^{-1}$  of UV irradiation. Results indicate that the AB113 removal efficiency increases from 80.3 to 99.6% when the Oxone dosage increases from 0.21 to 6.3 mM for 30 min of reaction time. From the results, the higher the Oxone dosage applies to the system, the higher AB113 removal efficiency can be approached. From Eq. (1), the more PMS is applied to a photoreactor with UV irradiation, the higher sulfate radical concentration will be produced. And sulfate radicals further react with AB113 to degrade AB113 structure. Similar observations for UV/PS system were obtained by Yang et al. for Acid Orange 7 at 200–2,000  $\text{mg l}^{-1}$  (0.84–8.4 mM) PS dosage and Kamel et al. for Congo red dye at 1.0–2.0 mM PS dosage [26,35].

In order to evaluate the effect of Oxone dosage on the AB113 degradation, two indicators are applied, that is, initial rate for first 2 min ( $\text{mg l}^{-1} \text{ min}^{-1}$ ) and removal efficiency at 30 min (%) which are summarized in Fig. 2(b). As shown in the figure, the initial rate increases exponentially with increase of Oxone dosage. And for Oxone dosage higher than 3.0 mM, the initial rate remains barely changed. Thus, an empirical equation as follows can be used to predict the initial rate ( $r_0$ , in  $\text{mg l}^{-1} \text{ min}^{-1}$ ) with known Oxone dosage ( $D$ , in mM).

$$r_0 = 5.569 + 14.105 \times (1 - e^{-1.0567 \times D}) \quad (2)$$

where  $r_0$  denotes the initial rate ( $\text{mg l}^{-1} \text{ min}^{-1}$ ) of AB113 degradation, and  $D$  is the Oxone dosage (mM).

Similarly, removal efficiency at 30 min also increases exponentially while Oxone dosage increasing. Another equation (Eq. (3)) is derived to express the effect of Oxone dosage on removal efficiency as follows:

$$R\%_{30\text{min}} = 77.346 + 22.828 \times (1 - e^{-0.6644 \times D}) \quad (3)$$

where  $R\%_{30\text{min}}$  denotes the B113 removal efficiency (%) at 30-min reaction time.  $D$  is the Oxone dosage (mM).

The effect of Oxone dosage on TOC removal efficiency under UV/Oxone process is demonstrated in Fig. 2(c). In this figure, the TOC removal efficiency presents a lag phase. For example, for Oxone dosage of 6.3 mM, there is a 10-min lag for TOC degradation. For Oxone dosage of 4.2 mM, a 30-min lag is observed for TOC mineralization. After this lag phase, the TOC concentration decreases sharply. As for lower Oxone dosage of 2.1 mM, the lag phase extends up to 60 min, then, TOC decreases slowly to about 18% removal. However, for the lowest Oxone dosage of 0.21 and 1.05 mM, TOC remains almost unchanged during 120 min of reaction time. From the figure, the TOC removal is 18% for Oxone dosage of 2.1 mM and increases up to 99.1% for Oxone dosage of 6.3 mM. Results indicate that the TOC removal is more sensitive to Oxone dosage than that of AB113 removal. To decolorize and mineralize simultaneously, one should choose higher Oxone dosage to full fill both AB113 dye and TOC removal requirements.

The reaction kinetics of AB113 degradation under UV/Oxone process is proved to follow pseudo-second-order reaction as shown in Fig. 2(d), and can be described as follows:

$$\frac{1}{C} = \frac{1}{C_0} + kt \quad (4)$$

where  $k$  denotes the pseudo-second-order reaction rate constant ( $\text{l mg}^{-1} \text{ min}^{-1}$ ),  $t$  is the reaction time (min),  $C_0$  designates the initial concentration ( $\text{mg l}^{-1}$ ) of AB113 and  $C$  is the concentration ( $\text{mg l}^{-1}$ ) of AB113, at time  $t$ .

The curve fitting of experimental results by Eq. (4) can be used to obtain rate constants. The rate constants follow similar trend as AB113 removal

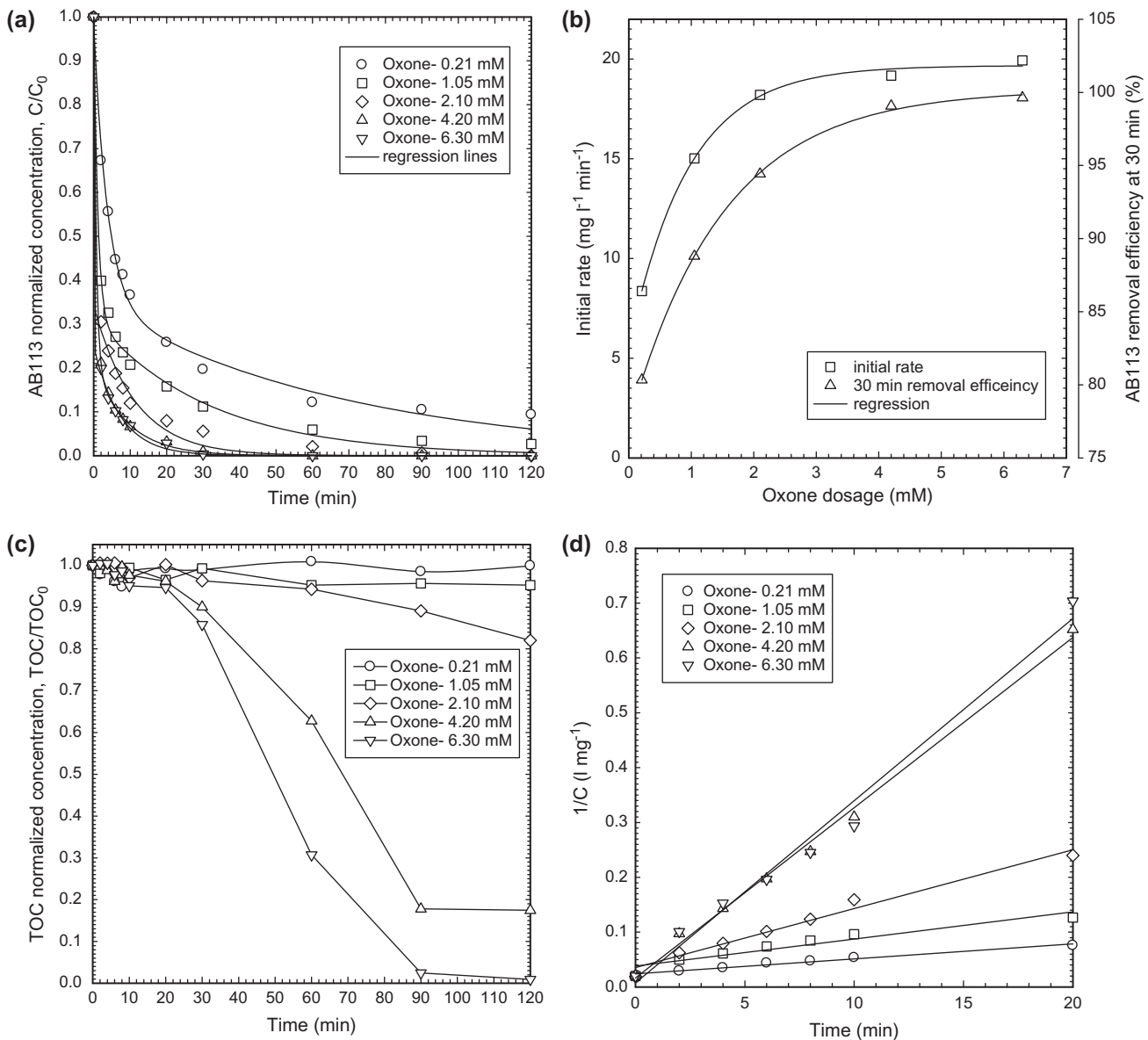


Fig. 2. Effect of Oxone dosage on (a) AB113 removal, (b) initial rate and 30 min removal efficiency, (c) TOC removal, and (d) second-order kinetics, by UV/Oxone system. The conditions were initial dye concentration of  $50 \text{ mg l}^{-1}$ , UV light intensity of  $30 \text{ W l}^{-1}$ , and reaction time during 120 min.

efficiency; the curve fitting calculated pseudo-second-order rate constants are  $0.0029$ ,  $0.0049$ ,  $0.0107$ ,  $0.0310$ , and  $0.0332 \text{ l mg}^{-1} \text{min}^{-1}$  at Oxone dosage of  $0.21$ ,  $1.05$ ,  $2.10$ ,  $4.20$ , and  $6.30 \text{ mM}$ , respectively. Since most of the AOPs studies show their reaction kinetics as pseudo-first-order kinetics, the reference kinetics data obtained is the first order rate constant of  $0.0908 \text{ min}^{-1}$  for Cibacron Brilliant Yellow 3 dye reported by Yeber et al. [36].

The summarized results are shown in Fig. 2(d). Under Oxone dosage of  $0.21$  to  $6.3 \text{ mM}$ , the pseudo-

second-order rate constant presents increasing with Oxone dosage increasing. However, there is only very small improvement obtained for Oxone dosage increasing from  $4.2$  to  $6.3 \text{ mM}$ .

### 3.3. Effect of initial dye concentration

To present the effect of initial AB113 concentration on this UV/Oxone system, the operating parameters were designed for AB113 initial concentrations of  $50$ – $400 \text{ mg l}^{-1}$ , Oxone dosage of  $6.3 \text{ mM}$

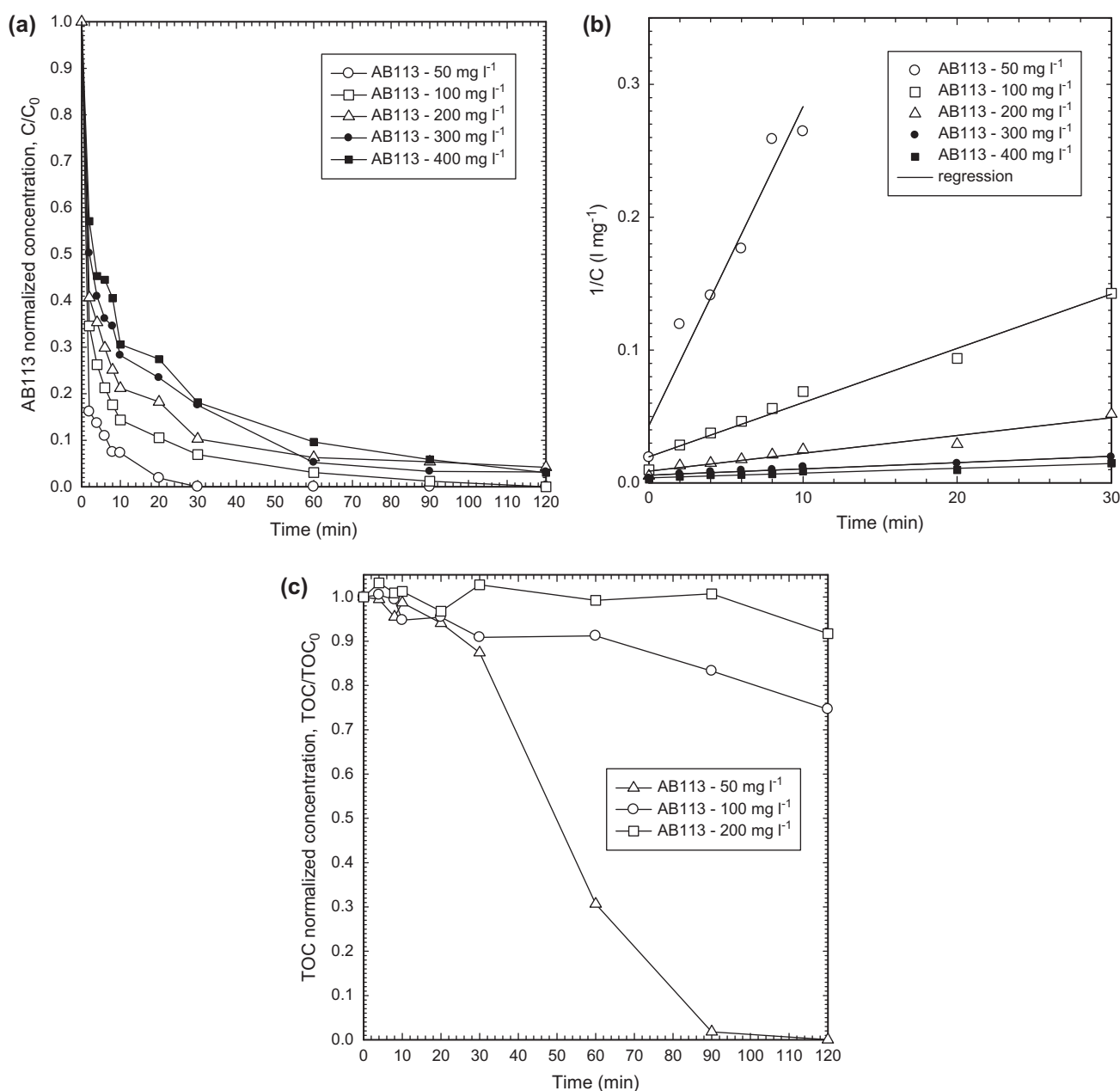


Fig. 3. Effect of initial concentration on (a) AB 113 degradation, (b) pseudo-second-order kinetics, and (c) TOC degradation. The operating conditions were Oxone dosage 6.3 mM, UV dosage of 30 W l<sup>-1</sup>, and reaction time 120 min.

and 30 W l<sup>-1</sup> UV dosage for a period of 120 min in the photoreactor. Fig. 3(a) presents results of AB113 photo-degradation as a function of reaction time at various initial dye concentrations. The second-order kinetics curves are presented in Fig. 3(b). Results indicate that the pseudo-second-order rate constant of dye removal decreases from 0.024 to  $4.0 \times 10^{-4}$  (l mg<sup>-1</sup> min<sup>-1</sup>) when the initial dye concentration increases from 50 to 400 mg l<sup>-1</sup> as calculated by

linear regression from Fig. 3(b). As shown in Fig. 3(c), the TOC removal efficiencies are 99.98, 25.35, and 8.27% in 120 min for initial AB113 concentration of 50, 100, and 200 mg l<sup>-1</sup>, respectively. For AB113 initial concentration higher than 300 mg l<sup>-1</sup>, almost no TOC degradation was observed. Results indicate that the TOC removal is more sensitive to initial AB113 concentration in comparison with AB113 removal.

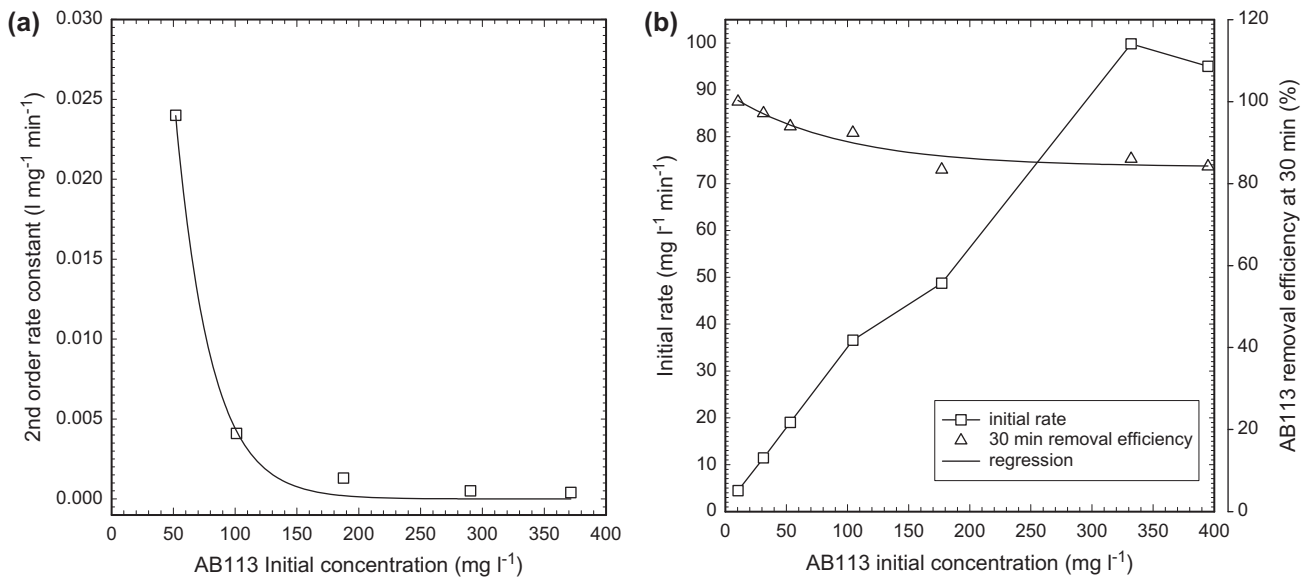


Fig. 4. Effect of AB113 initial concentration on (a) pseudo-second-order rate constant and (b) initial rate and 30 min removal efficiency of AB113 degradation by UV/Oxone system. The operating conditions were same as Fig. 3.

In Fig. 4(a), it is interesting to find that pseudo-second-order rate constant,  $k$ , declines exponentially by raising initial dye concentration while UV intensity of  $30\ W\ l^{-1}$ . An empirical equation can be obtained from this figure to present the effect of AB113 initial concentration on second-order rate constant.

$$k_{2nd} = 0.149 \times e^{-0.0352C_0} \quad (5)$$

where  $k_{2nd}$  denotes the second-order rate constant ( $l\ mg^{-1}\ min^{-1}$ ) at 30-min reaction time.  $C_0$  is the AB113 initial concentration ( $mg\ l^{-1}$ ).

The results are similar to the observations by other investigators that the declining pseudo-first-order rate constants with respect to increasing initial dye concentrations [10].

Similar to the effect of Oxone dosage treatment, initial rate ( $mg\ l^{-1}\ min^{-1}$ ) and removal efficiency at 30 min (%) are summarized in Fig. 4(b). As shown in the figure, the initial rate increases almost linearly to  $99.86\ mg\ l^{-1}\ min^{-1}$  with increasing of AB113 initial concentration up to  $300\ mg\ l^{-1}$ . Then, slightly drops down to  $95.02\ mg\ l^{-1}\ min^{-1}$  for  $400\ mg\ l^{-1}$  initial concentration. At higher initial AB113 concentration of  $400\ mg\ l^{-1}$ , there are abundant amount of AB113 dye molecules to react with sulfate radicals at initial stage of first 2 min and result in higher initial rate. Removal efficiency at 30 min decreases exponentially while AB113 initial concentration increases. However, the

range of removal efficiency at 30 min is fairly narrow from 84.2 to 100%. An equation can be derived to express the effect of AB113 initial concentration on removal efficiency at these operating conditions as follows.

$$R\%_{30min} = 54.068 + 18.176 \times (1 - e^{-0.0108C_0}) \quad (6)$$

where  $R\%_{30min}$  denotes the AB113 removal efficiency (%) at 30-min reaction time.  $C_0$  is the AB113 initial concentration ( $mg\ l^{-1}$ ).

### 3.4. Effect of pH

Fig. 5(a) shows AB 113 removal as a function of time at various pH values. Results indicate that at original pH of 5.8 the color removal reached 92.7% in 10 min of UV/Oxone reaction. At acidic pH of 2, the AB113 removal efficiency of 93.2% is obtained. This implies that acidic pH provides no benefit for AB113 degradation under UV/Oxone system. On the other hand, at alkaline pH of 10, the color removal efficiency slightly increased to 94.8%. However, the solution initial pH presents insignificant effect on AB113 degradation under UV/Oxone system. As shown in Fig. 5(b), results demonstrate that the best TOC removal at original pH 5.8 reaches 99.97% in 120 min of UV/Oxone reaction. At acidic pH of 2, the TOC removal efficiency of 0% at 30 min increases to 37.4% at 120-min reaction time. The pH 2, 7, and 10 conditions show

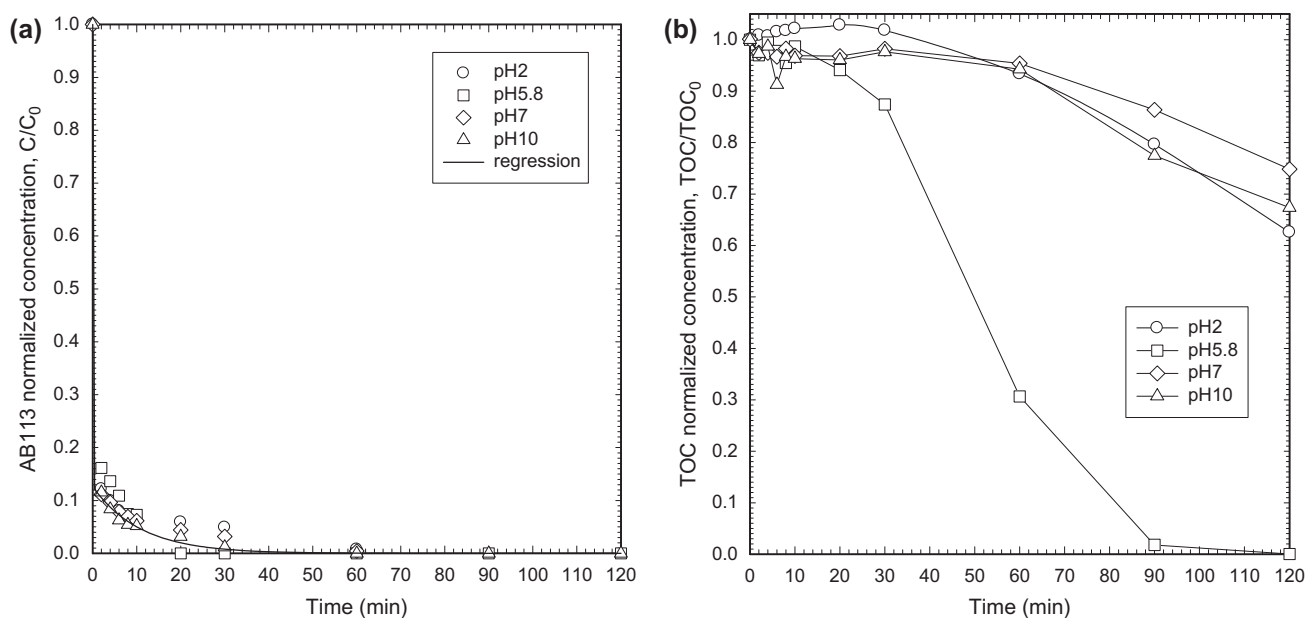


Fig. 5. Effect of initial pH on (a) AB113 degradation and (b) TOC mineralization under UV/Oxone system. The conditions were initial dye concentration of  $50 \text{ mg l}^{-1}$ , Oxone dosage  $6.3 \text{ mM}$ , UV dosage of  $30 \text{ W l}^{-1}$ , and reaction time during 120 min.

similar TOC removal behavior. The results imply various pH conditions resulting almost same AB113 decolorization. In contrast, the TOC removal efficiency is more influenced by various pH conditions. The original pH of 5.8 presents best TOC mineralization effect for UV/Oxone system to decompose AB113.

### 3.5. Effect of UV light intensity

Theoretically, the higher the UV light intensity applies to a photocatalytic system, the faster the  $\text{SO}_4^{\cdot-}$  free radical formation to obtain the higher dye decolorization and mineralization rate. Therefore, the rate constant increases by UV intensity increasing, while the same Oxone dosage applied. Because the photolysis of Oxone is enhanced by higher UV intensity, therefore, abundant  $\text{SO}_4^{\cdot-}$  free radicals in the dye solution are produced to degrade AB113 molecular structure. From the above theory, it implies that the more UV intensity employs to the UV/Oxone system, the faster is the dye decomposed. To verify this hypothesis, a voltage regulator was employed to adjust the 30 W UV lamp output to various intensities of  $2.0\text{--}5.6 \text{ mW cm}^{-2}$ . The UV 254 nm intensities were measured at the surface of quartz shell with a UV radiometer. Furthermore, another 14 W UV lamp was also conducted into this UV/Oxone experiments to evaluate UV effectiveness. Fig. 6(a) presents the removal of AB113 as a function of UV intensity for

$6.3 \text{ mM}$  Oxone dosage. Results demonstrate that at designated  $6.3 \text{ mM}$  Oxone dosage, the AB113 removal increases from 93.5 to 100% in 30 min when the UV intensity increases from  $2.0$  to  $5.6 \text{ mW cm}^{-2}$ . As reaction time increased up to 120 min, the AB113 removal efficiencies for various UV intensities are closer from 98 to 100% range. The results conclude that UV intensity contributes nearly no effect on AB113 degradation, the AB113 removal efficiencies are very close during whole reaction period as shown in the figure. In contrast, the mineralization of TOC depends on UV intensity significantly. As shown in Fig. 6(b), the mineralization of AB113 is thoroughly when Oxone dosage of  $6.3 \text{ mM}$  is applied for both  $4.0$  and  $5.6 \text{ mW cm}^{-2}$  UV intensities can reach 100% mineralization in 120 min. However, for the lowest UV intensity ( $2.0 \text{ mW cm}^{-2}$ ), the final TOC removal reaches only 9.9%. The results indicate that UV intensity factor is more important to the TOC mineralization than that of AB113 degradation. To verify this effect, a smaller UV lamp of 14 W was equipped into the UV/Oxone system to replace the original 30-W lamp. In this set of experiments,  $1.0 \text{ l}$  of  $50 \text{ mg l}^{-1}$  AB113 solution was pumped and recirculated through two different powered UV lamps to remain two different UV dosages of  $14$  and  $30 \text{ W l}^{-1}$ . From summarized Fig. 7, it is easy to observe that different UV dosages make litter differences between AB113 removal curves. In another word, UV dosage is not an important

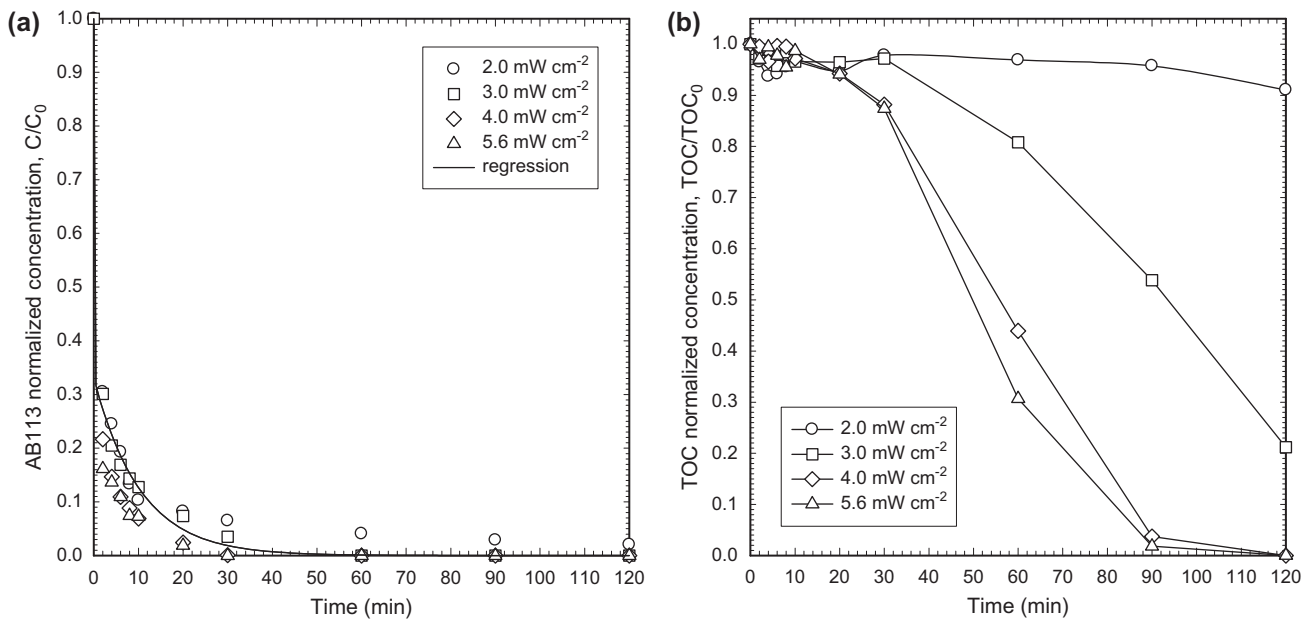


Fig. 6. Effect of UV intensity on (a) AB 113 degradation and (b) mineralization under UV/Oxone system. The conditions were initial dye concentration of  $50 \text{ mg l}^{-1}$ , Oxone dosage  $6.3 \text{ mM}$ , light intensity of  $2.0\text{--}5.6 \text{ mW cm}^{-2}$ , and reaction time during 120 min.

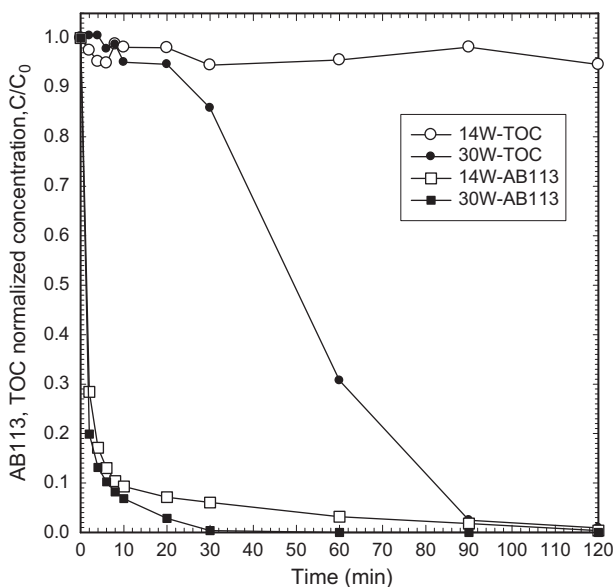


Fig. 7. Effect of UV dosage on AB113 degradation and TOC mineralization under UV/Oxone system. The conditions were initial dye concentration of  $50 \text{ mg l}^{-1}$ , Oxone dosage  $6.3 \text{ mM}$ , UV dosage of  $14\text{--}30 \text{ W l}^{-1}$ , and reaction time 120 min.

operating parameter for AB113 removal. As for TOC mineralization, different outcomes are obtained. The higher UV dosage ( $30 \text{ W l}^{-1}$ ) reaches the higher TOC

mineralization efficiency. On the other hand, for the lower dosage ( $14 \text{ W l}^{-1}$ ), the TOC mineralization was barely happened.

Due to the limitation of experimental setup, few previous works reported the effect of UV intensity on the decolorization of azo dye by UV/PS process. Salari et al. used an annular photoreactor with constant volumetric flow of  $500 \text{ ml min}^{-1}$  and adjustable UV intensity from  $5.5$  to  $40 \text{ W m}^{-1}$  to treat basic yellow 2 dye with a PS dosage of  $5 \text{ mM}$ . They reported that the decolorization rate increased with increasing light intensity. This outcome is consistent with the mineralization behavior of TOC in this work, but different from AB113 degradation results [37].

#### 4. Conclusions

UV/Oxone system, one of the SR-AOPs is demonstrated to be a powerful treatment technology for degradation and mineralization of AB113 wastewater. The Oxone dosage is presented to be most effective parameter to influence the AB113 and TOC removal efficiencies among all operating parameters studied. This proposed system can degrade AB113 with very high concentration up to  $400 \text{ mg l}^{-1}$ . However, the TOC mineralization for high AB113 concentration is so poor which needs longer reaction time and higher Oxone addition. For Oxone dosage from  $0.21$  to

6.3 mM, the higher the Oxone dosage applies, the higher the AB113 and TOC removal efficiencies can be obtained. For Oxone dosage less than 2.1 mM, no significant TOC mineralization is observed. The UV intensity affects TOC mineralization more demonstrably than degradation of AB113. UV intensity larger than 3.0 mW cm<sup>-2</sup> presents significant TOC mineralization. The initial pH is demonstrated to be less effective on the AB113 degradation. However, the original pH of 5.8 shows best TOC mineralization. The degradation of AB113 presents pseudo-second-order kinetics. This result shows very different conclusion in comparison with other AOPs applications of pseudo-first-order kinetics.

### Acknowledgements

The authors appreciate the research funding granted by the Taiwan Ministry of Science and Technology (MOST101-2221-E-241-004-MY3).

### References

- [1] Taiwan Ministry of Finance, Brief Export-import Statistic Monthly, Available from: <<http://www.mof.gov.tw/ct.asp?xItem=78850&ctNode=2449>>, Accessed 2015/1/31.
- [2] C.M. Kao, M.S. Chou, W.L. Fang, B.W. Liu, B.R. Huang, Regulating colored textile wastewater by 3/31 wavelength admittance methods in Taiwan, *Chemosphere* 44 (2001) 1055–1063.
- [3] A. Aris, P.N. Sharratt, Fenton oxidation of reactive black 5: Effect of mixing intensity and reagent addition strategy, *Environ. Technol.* 25 (2004) 601–612.
- [4] N.N. Rao, G. Bose, P. Khare, S.N. Kaul, Fenton and electro-Fenton methods for oxidation of H-acid and reactive black 5, *J. Environ. Eng.* 132 (2006) 367–376.
- [5] H.Y. Shu, Degradation of dye house effluent containing C.I. Direct Blue 199 by processes of ozonation, UV/H<sub>2</sub>O<sub>2</sub> and in sequence of ozonation with UV/H<sub>2</sub>O<sub>2</sub>, *J. Hazard. Mater.* 133 (2006) 92–98.
- [6] Y.H. Huang, S.T. Tsai, Y.F. Huang, C.Y. Chen, Degradation of commercial azo dye reactive black B in photo/ferrioxalate system, *J. Hazard. Mater.* 140 (2007) 382–388.
- [7] P. Cañizares, A. Gadri, J. Lobato, B. Nasr, R. Paz, M.A. Rodrigo, C. Saez, Electrochemical oxidation of azoic dyes with conductive-diamond anodes, *Ind. Eng. Chem. Res.* 45 (2006) 3468–3473.
- [8] M.A. Behnajady, N. Modirshahla, N. Daneshvar, M. Rabbani, Photocatalytic degradation of C.I. Acid Red 27 by immobilized ZnO on glass plates in continuous-mode, *J. Hazard. Mater.* 140 (2007) 257–263.
- [9] M. Muruganandham, N. Shobana, M. Swaminathan, Optimization of solar photocatalytic degradation conditions of Reactive Yellow 14 azo dye in aqueous TiO<sub>2</sub>, *J. Mol. Catal. A: Chem.* 246 (2006) 154–161.
- [10] H.Y. Shu, M.C. Chang, H.J. Fan, Effects of gap size and UV dosage on decolorization of C.I. Acid Blue 113 wastewater in the UV/H<sub>2</sub>O<sub>2</sub> process, *J. Hazard. Mater.* 118 (2005) 205–211.
- [11] H.Y. Shu, M.C. Chang, Pre-ozonation coupled with UV/H<sub>2</sub>O<sub>2</sub> process for the decolorization and mineralization of cotton dyeing effluent and synthesized C.I. Direct Black 22 wastewater, *J. Hazard. Mater.* 121 (2005) 127–133.
- [12] S.D. Kalpana, C. Kalyanaraman, N.N. Gandhi, Application of H<sub>2</sub>O and UV/H<sub>2</sub>O<sub>2</sub> processes for enhancing the biodegradability of reactive black 5 dye, *J. Environ. Sci. Eng.* 53 (2011) 271–276.
- [13] M.C. Chang, H.Y. Shu, H.H. Yu, An integrated technique using zero-valent iron and UV/H<sub>2</sub>O<sub>2</sub> sequential process for complete decolorization and mineralization of C.I. Acid Black 24 wastewater, *J. Hazard. Mater.* 138 (2006) 574–581.
- [14] H.Y. Shu, M.C. Chang, Pilot scale annular plug flow photo reactor by UV/H<sub>2</sub>O<sub>2</sub> for the decolorization of azo dye wastewater, *J. Hazard. Mater.* 125 (2005) 244–251.
- [15] H.Y. Shu, M.C. Chang, Decolorization effects of six azo dyes by O<sub>3</sub>, UV/O<sub>3</sub> and UV/H<sub>2</sub>O<sub>2</sub> processes, *Dyes Pigment.* 65 (2005) 25–31.
- [16] G. Ersöz, Fenton-like oxidation of Reactive Black 5 using rice husk ash based catalyst, *Appl. Catal., B* 147 (2014) 353–358.
- [17] S. Sakthivel, B. Neppolian, M.V. Shankar, B. Arabindoo, M. Palanichamy, V. Murugesan, Solar photocatalytic degradation of azo dye: Comparison of photocatalytic efficiency of ZnO and TiO<sub>2</sub>, *Sol. Energy Mater. Sol. Cells* 77 (2003) 65–82.
- [18] W.L. Kostedt IV, A.A. Ismail, D.W. Mazyck, Impact of heat treatment and composition of ZnO–TiO<sub>2</sub> nanoparticles for photocatalytic oxidation of an azo dye, *Ind. Eng. Chem. Res.* 47 (2008) 1483–1487.
- [19] M.C. Chang, C.P. Huang, H.Y. Shu, Y.C. Chang, A new photocatalytic system using steel mesh and cold cathode fluorescent light for the decolorization of azo dye orange G, *Int. J. Photoenergy* 2012 (2012) 1–9.
- [20] M.C. Chang, H.Y. Shu, T.H. Tseng, H.W. Hsu, Supported zinc oxide photocatalyst for decolorization and mineralization of orange G dye wastewater under UV365 irradiation, *Int. J. Photoenergy* 2013 (2013) 1–9.
- [21] S.C. Fang, S.L. Lo, Persulfate oxidation activated by peroxide with and without iron for remediation of soil contaminated by heavy fuel oil: Laboratory and pilot-scale demonstrations, *Appl. Mech. Mater.* 121–126 (2012) 2546–2556.
- [22] M.L. Crimi, J. Taylor, Experimental evaluation of catalyzed hydrogen peroxide and sodium persulfate for destruction of BTEX contaminants, *Soil Sediment Contam.* 16 (2007) 29–45.
- [23] S.Y. Oh, S.G. Kang, P.C. Chiu, Degradation of 2,4-dinitrotoluene by persulfate activated with zero-valent iron, *Sci. Total Environ.* 408 (2010) 3464–3468.
- [24] C.H. Yen, K.F. Chen, C.M. Kao, S.H. Liang, T.Y. Chen, Application of persulfate to remediate petroleum hydrocarbon-contaminated soil: Feasibility and comparison with common oxidants, *J. Hazard. Mater.* 186 (2011) 2097–2102.
- [25] R.H. Waldemer, P.G. Tratnyek, R.L. Johnson, J.T. Nurmi, Oxidation of chlorinated ethenes by heat-activated persulfate: Kinetics and products, *Environ. Sci. Technol.* 41 (2007) 1010–1015.

- [26] S. Yang, P. Wang, X. Yang, L. Shan, W. Zhang, X. Shao, R. Niu, Degradation efficiencies of azo dye acid orange 7 by the interaction of heat, UV and anions with common oxidants: Persulfate, peroxymonosulfate and hydrogen peroxide, *J. Hazard. Mater.* 179 (2010) 552–558.
- [27] J. Sun, X. Li, J. Feng, X. Tian, Oxone/ $\text{Co}^{2+}$  oxidation as an advanced oxidation process: Comparison with traditional Fenton oxidation for treatment of landfill leachate, *Water Res.* 43 (2009) 4363–4369.
- [28] M. Mahdi-Ahmed, S. Chiron, Ciprofloxacin oxidation by UV-C activated peroxymonosulfate in wastewater, *J. Hazard. Mater.* 265 (2014) 41–46.
- [29] J. Sun, M. Song, J. Feng, Y. Pi, Highly efficient degradation of ofloxacin by UV/Oxone/ $\text{Co}^{2+}$  oxidation process, *Environ. Sci. Pollut. Res.* 19 (2012) 1536–1543.
- [30] Y.R. Wang, W. Chu, Degradation of a xanthene dye by Fe(II)-mediated activation of Oxone process, *J. Hazard. Mater.* 186 (2011) 1455–1461.
- [31] Z. Wang, R. Yuan, Y. Guo, L. Xu, J. Liu, Effects of chloride ions on bleaching of azo dyes by  $\text{Co}^{2+}$ /oxone reagent: Kinetic analysis, *J. Hazard. Mater.* 190 (2011) 1083–1087.
- [32] H.Y. Shu, H.J. Fan, M.C. Chang, W.P. Hsieh, Treatment of MSW landfill leachate by a thin gap annular UV/ $\text{H}_2\text{O}_2$  photoreactor with multi-UV lamps, *J. Hazard. Mater.* 129 (2006) 73–79.
- [33] Honeywell International Inc., ORP Provides Versatile Water Treatment, Solution Note, SO-13-17-ENG, 2013.
- [34] Y.O. Kim, H.U. Nam, Y.R. Park, J.H. Lee, T.J. Park, T.H. Lee, Fenton oxidation process control using oxidation-reduction potential measurement for pigment wastewater treatment, *Korean J. Chem. Eng.* 21 (2004) 801–805.
- [35] D. Kamel, A. Sihem, C. Halima, S. Tahar, Decolourization process of an azoïque dye (Congo red) by photochemical methods in homogeneous medium, *Desalination* 247 (2009) 412–422.
- [36] M.C. Yeber, L. Díaz, J. Fernández, Catalytic activity of the  $\text{SO}_4^-$  radical for photodegradation of the azo dye Cibacron Brilliant Yellow 3 and 3,4-dichlorophenol: Optimization by application of response surface methodology, *J. Photochem. Photobiol., A* 215 (2010) 90–95.
- [37] D. Salari, A. Niaei, S. Aber, M.H. Rasoulifard, The photooxidative destruction of C.I. Basic Yellow 2 using UV/ $\text{S}_2\text{O}_8^{2-}$  process in a rectangular continuous photoreactor, *J. Hazard. Mater.* 166 (2009) 61–66.